1248 *Biochemistry* **2010,** *49,* 1248–1258
DOI: 10.1021/bi9019548

BIOCHEMISTRY
including biophysical chemistry & molecular biology
Article

Interaction of ATP with the Phosphoenzyme of the Na^+,K^+-ATPase[†]

Mohammed Khalid,[‡] Gaëlle Fouassier,[‡] Hans-Jürgen Apell,[§] Flemming Cornelius,[∥] and Ronald J. Clarke*,[‡]

[‡]*School of Chemistry, University of Sydney, Sydney, New South Wales 2006, Australia,* [§]*Faculty of Biology, University of Konstanz, D-78435 Konstanz, Germany, and* [∥]*Department of Physiology and Biophysics, University of Aarhus, DK-8000 Aarhus C, Denmark*

Received November 13, 2009; Revised Manuscript Received January 11, 2010

ABSTRACT: The interaction of ATP with the phosphoenzyme of Na^+,K^+-ATPase from pig kidney, rabbit kidney, and shark rectal gland was investigated using the voltage-sensitive fluorescent probe RH421. In each case, ATP concentrations ≥100 μM caused a drop in fluorescence intensity, which, because RH421 is sensitive to the formation of enzyme in the E2P state, can be attributed to ATP binding to the E2P phosphoenzyme. Simulations of the experimental behavior using kinetic models based on either a monomeric or a dimeric enzyme mechanism yielded a K_d for ATP binding in the range 140−500 μM. Steady-state activity measurements and independent measurements of the phosphoenzyme level via a radioactive assay indicated that ATP binding to E2P causes a deceleration in its dephosphorylation when acting in the Na^+-ATPase mode, i.e., in the absence of K^+ ions. Both the ATP-induced drop in RH421 fluorescence and the effect on the dephosphorylation reaction could be attributed to an inhibition of dissociation from the E2P$(Na^+)_3$ state of the one Na^+ ion necessary to allow dephosphorylation. Stopped-flow studies on the shark enzyme indicated that the ATP-induced inhibition of dephosphorylation is abolished in the presence of 1 mM KCl. A possible physiological role of allosteric binding of ATP to the phosphoenzyme could be to stabilize the E2P state and stop the enzyme running backward, which would cause dissipation of the Na^+ electrochemical potential gradient and the resynthesis of ATP from ADP. ATP binding to E2P could also fix ATP within the enzyme ready to phosphorylate it in the subsequent turnover.

The most widely used model of the mechanism of P-type ATPases is the Albers−Post or E1−E2 model (see Figure 1) (*1*, *2*). Although this model does not explain the kinetic behavior of these enzymes under all conditions, it does appear to be followed at high ATP[1] concentrations (i.e., millimolar range), and it is, thus, a useful starting point for discussion. In the case of the Na^+,K^+-ATPase the E2 → E1 transition of the unphosphorylated enzyme and its associated release of K^+ ions to the cytoplasm are dramatically accelerated by the presence of ATP (*3*). This acceleration is crucial to the enzyme under physiological conditions, because the E2 → E1 transition is one of the rate-determining steps of the enzyme's reaction cycle (*4*−*6*). Therefore, ATP plays a critical role in optimizing the rate of ion pumping as well as providing the necessary energy. The situation is similar in the case of the sarcoplasmic Ca^{2+}-ATPase from cardiac muscle (*7*).

In the case of sarcoplasmic Ca^{2+}-ATPase from *skeletal* muscle it has been found that ATP accelerates ion pumping by stimulating a different step of the cycle, i.e., the release of Ca^{2+} into the lumen of the sarcoplasmic reticulum. This must involve ATP binding to the phosphorylated form of the enzyme (*7*−*10*). It has also been found that the dephosphorylation reaction of the Ca^{2+}-ATPase is accelerated by ATP, which also necessitates ATP binding to the phosphorylated enzyme (*10*, *11*). Thus, these results indicate that phosphorylation and ATP binding without phosphorylation are not mutually exclusive reactions for P-type ATPases; i.e., the enzymes can exist in a state in which they are simultaneously phosphorylated and have bound ATP. This result from kinetic measurements has recently been supported by X-ray crystallographic studies showing a crystal structure of the sarcoplasmic reticulum Ca^{2+}-ATPase with bound ADP and the phosphate analogue AlF_4^-, which represents an E1∼PADP transition state (*12*), and another crystal structure with the nonhydrolyzable ATP derivative AMPPCP bound together with AlF_4^-, representing an E2P−ATP state (*13*).

Because the Na^+,K^+-ATPase and the sarcoplasmic reticulum Ca^{2+}-ATPase are closely related enzymes, it may also be the case that ATP binding occurs to phosphorylated Na^+,K^+-ATPase. However, up to now only three crystal structures of the Na^+,K^+-ATPase have been published, and none are in a covalently phosphorylated form (*14*−*16*). Therefore, there are no structural data available to support a phosphorylated state of the Na^+,K^+-ATPase with a bound nucleotide. Kinetic data are also so far inconclusive. Askari and Huang (*17*) found that ATP reduced the rate of dephosphorylation of phosphoenzyme previously produced by phosphorylation with inorganic phosphate. Post et al. (*18*) had also earlier found a slight reduction in dephosphorylation rate by ADP, but they did not extend their studies to a sufficiently high concentration to determine a $K_{0.5}$. Askari and Huang (*17*) determined a $K_{0.5}$ for this effect of around 0.2 mM from their measurements. This value is similar to the

[†]This work was supported by the Australian Research Council/National Health and Medical Research Council funded Research Network "Fluorescence Applications in Biotechnology and Life Sciences" (RN0460002).

*To whom correspondence should be addressed. Phone: +61 2 9351 4406. Fax: +61 2 9351 3329. E-mail: r.clarke@chem.usyd.edu.au.

[1]Abbreviations: Na^+,K^+-ATPase, sodium and potassium ion-activated adenosine triphosphatase; Ca^{2+}-ATPase, calcium ion-activated adenosine triphosphatase; ATP, adenosine 5′-triphosphate; ADP, adenosine 5′-diphosphate; E1, E2, E1P, and E2P, intermediates of the Na^+,K^+-ATPase pump cycle; RH421, *N*-(4-sulfobutyl)-4-(4-(*p*-(dipentylamino)phenyl)butadienyl)pyridinium inner salt.

 Published on Web 01/11/2010

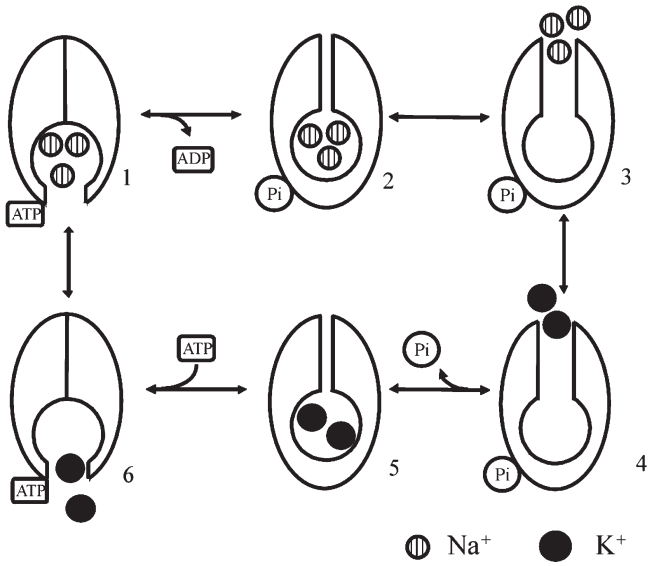

FIGURE 1: Albers−Post or E1−E2 model of the mechanism of P-type ATPases (shown for the Na^+,K^+-ATPase). The sequence of intermediates from 1 to 6 around the cycle correspond to the following reactions: $E1(Na^+)_3ATP \rightarrow E2P(Na^+)_3 \rightarrow E2P \rightarrow E2P\text{-}(K^+)_2 \rightarrow E2(K^+)_2 \rightarrow E1(K^+)_2$. The diagram has been modified from ref *2*.

K_d for regulatory binding of ATP to the unphosphorylated E2 form of the enzyme, which has been reported to have a value in the range 0.07−0.5 mM (*4*, *19*−*23*). At the time, Askari and Huang (*17*) interpreted their data as indicating that the enzyme possessed two ATP sites on its functional unit. This conclusion, however, was based on the assumption that the ATP binding site and the phosphorylation site are in such close proximity to one another that ATP binding and phosphorylation would be mutually exclusive reactions. As discussed above, this assumption has been shown for the skeletal muscle sarcoplasmic reticulum Ca^{2+}-ATPase to be unjustified. More recent studies by Clarke and Kane (*24*) using enzyme isolated from pig kidney and the voltage-sensitive fluorescent probe RH421, which is known to respond to the release of Na^+ from the $E2P(Na^+)_3$ state with an increase in fluorescence, showed a drop in the magnitude of the fluorescence increase of the probe at high ATP concentrations. This result was interpreted as being due to a binding of ATP to the E2P state, which was suggested (*24*) to cause a decrease in the accumulation of enzyme in the E2P state under steady-state conditions due to an acceleration of the dephosphorylation reaction by ATP, i.e., apparently the opposite effect to that found by Askari and Huang (*17*). Nevertheless, the K_d reported for ATP binding to the E2P state by Clarke and Kane (*24*) of 0.14 mM was very similar to that found by Askari and Huang (*17*). An alternative explanation for the results observed by Clarke and Kane (*24*) could be that ATP binding to the E2P state influences the fluorescence level of bound RH421 without accelerating the rate constant for dephosphorylation. Therefore, to clarify this situation, the aims of this paper are to determine whether or not ATP has any effect on the dephosphorylation of the Na^+,K^+-ATPase, if so, whether the effect is present in both the Na^+-ATPase and Na^+,K^+-ATPase modes of the enzyme, and, in general, to determine what role ATP has in the reactions of the phosphoenzyme of the Na^+,K^+-ATPase. A further important point is that, in order to explain their data from pig kidney enzyme, Clarke and Kane (*24*) needed to assume that at low ATP concentrations the enzyme existed in a dimeric form $(\alpha\beta)_2$ within the membrane. To judge whether this is generally the case, we have extended the studies here to two further preparations, rabbit kidney and shark rectal gland.

MATERIALS AND METHODS

Enzyme and Reagents. Na^+,K^+-ATPase-containing membrane fragments from shark rectal glands were purified as described by Skou and Esmann (*25*). The specific ATPase activity at 37 °C and pH 7.4 was measured according to Ottolenghi (*26*). The activity of the preparation used was 1765 μmol of ATP hydrolyzed h^{-1} (mg of protein)$^{-1}$ at saturating substrate concentrations and the protein concentration was 6.8 mg mL^{-1}. The concentration was determined according to the Peterson modification (*27*) of the Lowry method (*28*) using bovine serum albumin as a standard. For the calculation of the molar protein concentration, a molecular mass for an $\alpha\beta$ unit of the Na^+,K^+-ATPase of 147000 g mol^{-1} (*29*) was used.

Na^+,K^+-ATPase-containing membrane fragments from the red outer medulla of rabbit and pig kidney were purified according to a modification (*30*) of procedure C of Jørgensen (*31*, *32*). The specific activity of the pig preparation was ~1800 μmol of ATP hydrolyzed h^{-1} (mg of protein)$^{-1}$ for the pig kidney preparation at saturating substrate concentrations, and its concentration was 2 mg/mL. For the rabbit preparation the activity was 2106 μmol of ATP hydrolyzed h^{-1} (mg of protein)$^{-1}$ at saturating substrate concentrations, and its protein concentration was 2.1 mg/mL. The enzymatic activities in the presence of 1 mM ouabain were < 1%. The concentrations of both of these preparations were determined by the Lowry method (*28*). The enzymatic activities were determined by the pyruvate kinase/lactate dehydrogenase coupled enzyme assay (*33*).

N-(4-Sulfobutyl)-4-(4-(*p*-(dipentylamino)phenyl)butadienyl)-pyridinium salt (RH421) was obtained from Molecular Probes (Eugene, OR) and was used without further purification. RH421 was added to Na^+,K^+-ATPase-containing membrane fragments from an ethanolic stock solution. The dye is spontaneously incorporated into the membrane fragments.

The origins of the various reagents used were as follows: imidazole (≥99%; Sigma, Castle Hill, Australia), NaCl (suprapure; Merck, Kilsyth, Australia), $MgCl_2 \cdot 6H_2O$ (analytical grade; Merck), EDTA (99%; Sigma), $Na_2ATP \cdot 3H_2O$ (special quality; Boehringer-Mannheim, Mannheim, Germany, or Roche, Castle Hill, Australia), [γ-^{32}P]ATP disodium salt (Amersham, Little Chalfont, U.K.), trichloroacetic acid (analytical grade; Merck) sodium pyrophosphate decahydrate (analytical grade; Merck), phosphoric acid (analytical grade; Merck), NaOH (analytical grade; Merck), and HCl (0.1 N Titrisol solution; Merck). The radioactively labeled disodium ATP was freed of ADP and converted into a tris salt on a DEAE-Sephadex A-25 column (*34*) before reacting it with the Na^+,K^+-ATPase.

Stopped-Flow Spectrofluorometry. Stopped-flow experiments were carried out on Na^+,K^+-ATPase-containing membrane fragments from pig kidney or shark rectal gland using an SF-61 stopped-flow spectrofluorometer from Hi-Tech Scientific (Salisbury, U.K.). Measurements of the kinetics of the Na^+-ATPase exchange mode of the enzyme were carried out as described previously (*24*). The amplitudes ($\Delta F/F_0$) of the RH421 fluorescence changes associated with the Na^+,K^+-ATPase conformational changes and ion translocation reactions were investigated at 24 °C in the stopped-flow apparatus by mixing Na^+,K^+-ATPase (labeled with RH421) with an equal volume of

an ATP solution from the other drive syringe. To improve the signal-to-noise ratio, typically between 6 and 14 experimental traces were averaged before the amplitude was evaluated. The magnitudes of the amplitudes were determined from nonlinear least-squares fits of either one or a sum of two exponential functions to the averaged experimental trace. The solutions in each of the drive syringes were prepared in a buffer containing 30 mM imidazole, 130 mM NaCl, 5 mM $MgCl_2$, and 1 mM EDTA, so that no change in the Na^+ concentration occurred on mixing.

Measurements of the kinetics of K^+-induced dephosphorylation of the enzyme were carried out as described previously (*35*). Briefly, Na^+,K^+-ATPase-containing membrane fragments (20 μg/mL of enzyme) from shark rectal gland, labeled with RH421 (300 nM), were premixed in one of the drive syringes with varying volumes of 35 mM Na_2ATP to final ATP concentrations in the range 50−7000 μM. After phosphorylation of the enzyme had reached a steady state (this occurs within 1 s), the enzyme was mixed with an equal volume of a solution of either 12, 2, or 0.5 mM KCl from the other drive syringe, so that the final K^+ concentration after mixing was either 6, 1, or 0.25 mM. The enzyme suspension and the KCl solution were prepared in the same buffer containing 30 mM imidazole, 130 mM NaCl, 5 mM $MgCl_2$, and 1 mM EDTA. The pH was adjusted to 7.4 by the addition of HCl. The KCl concentrations used were chosen based on previous studies (*35*) so as to cover both saturating and nonsaturating conditions of the extracellular K^+ binding sites.

Radioactive Measurement of Phosphorylation Levels. Phosphorylation of Na^+,K^+-ATPase from shark rectal gland by [γ-^{32}P]ATP (25 μM−2 mM) was performed as previously described (*36*). The enzyme was reacted with [γ-^{32}P]ATP for 20 s at 0 °C in a medium containing 4 mM $MgCl_2$, 150 mM NaCl, and 30 mM imidazole at pH 7.4 to obtain maximum phosphorylation. Phosphorylation was followed by protein precipitation at 0 °C in 10% (w/v) trichloroacetic acid and 100 mM phosphoric acid and washing twice with an ice-cold solution containing 0.1% (w/v) trichloroacetic acid, 10 mM phosphoric acid, and 10 mM pyrophosphate. Protein and radioactivity in the precipitate were determined after resuspension in 1 M NaOH at 55 °C. Protein concentrations were determined according to Peterson (*27*).

Fluorescence Measurements. Fluorescence measurements were carried out with either a Shimadzu RF-5301 PC spectrofluorophotometer or a Perkin-Elmer LS 50B fluorescence spectrophotometer. Quartz semimicro cuvettes were used for all measurements. The temperature was maintained at 24 °C using a circulating water bath connected to the sample holder. λ_{ex} was 570 nm (bandwidth 10 nm) with an OG530 cutoff filter (Schott) in the excitation path. λ_{em} was 670 nm (bandwidth 10 nm) with an RG645 cutoff filter (Schott) in front of the photomultiplier.

The relative fluorescence change, $\Delta F/F_0$, of membrane-bound RH421 associated with phosphorylation of the Na^+,K^+-ATPase by ATP and its conversion to the E2P state was determined by measuring the change in fluorescence, ΔF, of a suspension of Na^+,K^+-ATPase-containing membrane fragments labeled with RH421 following ATP addition using the spectrofluorophotometer in time-scan mode and then dividing ΔF by the fluorescence level prior to ATP addition, F_0.

Steady-State Activity Measurements. Steady-state activity measurements of the Na^+-ATPase activity of the Na^+,K^+-ATPase from shark rectal gland were carried out either by measuring the amount of ^{32}P released from [γ-^{32}P]ATP using the method of Lindberg and Ernster (*37*) (at ATP concentrations up to 1000 μM) or by using the spectrophotometric method of phosphate determination of Baginski et al. (*38*) (at ATP concentrations from 50 to 3000 μM). In both cases ATP was used as the tris salt. The buffer used for these measurements contained 30 mM histidine, 130 mM NaCl, and 5 mM $MgCl_2$. The pH was adjusted to pH 7.4 with HCl. The measurements were performed at 23 °C. The enzyme concentration and the test time were adjusted in order for hydrolysis not to exceed 20% of the added ATP.

Simulations. Computer simulations of the amplitude of the RH421 fluorescence change associated with ATP addition to the Na^+,K^+-ATPase-containing membrane fragments were performed using the commercially available program Berkeley Madonna 8.0 (University of California, Berkeley) via the variable step-size Rosenbrock integration method for stiff systems of differential equations. The simulations yield the time course of the concentration of each enzyme intermediate involved as well as the total fluorescence. For the purposes of the simulations, each enzyme intermediate was normalized to a unitary enzyme concentration.

RESULTS

Simulations of the Amplitudes of ATP-Induced Stopped-Flow Fluorescence Traces. The voltage-sensitive fluorescent dye RH421 is known to respond to the formation of enzyme in the E2P state with an increase in its fluorescence induced by the release of Na^+ to the extracellular side of the membrane (*39*−*41*). Therefore, it can be used to follow the time course of E2P formation from E1(Na^+)$_3$ (*24*) or the dephosphorylation of E2P on mixing with K^+ ions (*35*). In a previous stopped-flow kinetic study using this dye (*24*) we found that on mixing Na^+,K^+-ATPase in the presence of 130 mM NaCl and 5 mM $MgCl_2$ with increasing concentrations of Na_2ATP the relative fluorescence change ($\Delta F/F_0$) increased until it reached a maximum of around 0.95 at approximately 20 μM ATP. At higher ATP concentrations $\Delta F/F_0$ then decreased again. The experimental data from ref *24* is reproduced in Figure 2. In order to explain the observed behavior of both the amplitudes and the time courses of the kinetic traces over the entire ATP concentration range studied, we found that a dimer model of the Na^+,K^+-ATPase's mechanism was required (see Figure 3). Simpler monomeric or two-pool enzyme models were unable to explain the data. The dimer model of Figure 3 shows the mechanism in a linear branched format, although in fact it incorporates the entire reaction cycle of the enzyme. This is because the reverse reactions E2P:E1 → E1ATP:E1, E1:E2P → E1:E1ATP, and E2P:E2P → E1ATP:E1ATP with rate constants k_{-3}, k_{-3}, and k_{-4}, respectively, actually represent a sequence of reactions involving the enzyme continuing around its normal catalytic cycle, i.e., via dephosphorylation, the E2 → E1 transition, and finally binding of ATP. They are not meant to signify a direct re-formation of ATP by reaction of phosphorylated enzyme with ADP.

Because RH421 reports the conversion of enzyme in the E1(Na^+)$_3$ state to the E2P state, it was found (*24*) that the drop in $\Delta F/F_0$ at high ATP concentrations (> 20 μM) could in principle be explained by a drop in the proportion of enzyme in the $(E2P)_2$ state due to an increase in the rate constant of the dephosphorylation reaction relative to that of phosphorylation, whereby the acceleration of dephosphorylation could come about via ATP binding to the $(E2P)_2$ state, i.e., in an analogous fashion to the situation known to occur in the case of the

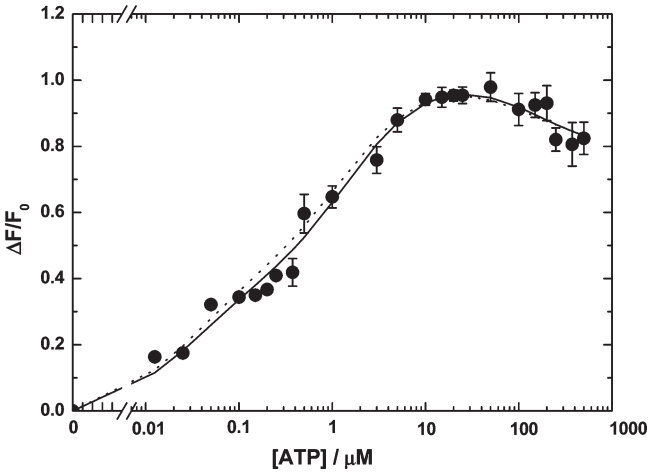

FIGURE 2: Amplitudes ($\Delta F/F_0$) of the total observed fluorescence change of stopped-flow fluorescence transients measured when pig Na^+,K^+-ATPase noncovalently labeled with RH421 was mixed with an equal volume of a solution containing varying concentrations of Na_2ATP (reproduced from ref *24*). The Na^+,K^+-ATPase and RH421 concentrations were 10 μg/mL (or 68 nM) and 75 nM. The enzyme suspension and the Na_2ATP solutions were prepared in buffer containing 130 mM NaCl, 30 mM imidazole, 5 mM $MgCl_2$, and 1 mM EDTA (pH 7.4, 24 °C). The fluorescence of membrane-bound RH421 was measured at λ_{ex} = 577 nm and $\lambda_{em} \geq$ 665 nm (RG665 glass cutoff filter). ΔF is the total fluorescence change (i.e., of both kinetic phases if a two-phase signal was observed), and F_0 is the initial fluorescence level before mixing with ATP. The dashed line represents the prediction of simulations based on a dimer model (see Figure 3) incorporating an acceleration of the dephosphorylation rate constant due to ATP binding to the E2P:E2P state (for mathematical details of this model see ref *24*). The solid line represents the prediction of simulations based on the same dimer model (see Figure 3) but incorporating an ATP-induced decrease in the fluorescence level of RH421 associated with the E2P:E2P state.

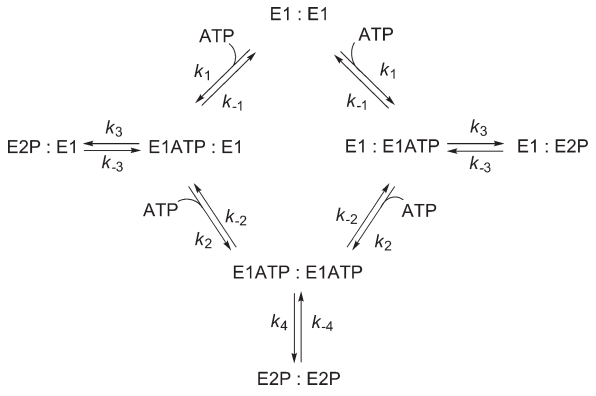

FIGURE 3: Reaction scheme of the dimer model of Na^+,K^+-ATPase phosphorylation by ATP.

sarcoplasmic reticulum Ca^{2+}-ATPase (*10*). However, if RH421 fluorescence is sensitive to Na^+ release from $E2P(Na^+)_3$, an alternative explanation of the drop in $\Delta F/F_0$ at high ATP concentrations could be that ATP binding to $(E2P)_2$ decreases the fluorescence level, $f_{(E2P)_2}$, of RH421 associated with the $(E2P)_2$ state, e.g., by a dose-dependent shift in the Na^+ dissociation/association equilibrium with E2P. This is mathematically expressed by the equation:

$$f_{(E2P)_2} = f_{(E2P)_2}{}^{max} + \left(f_{(E2P)_2}{}^{min} - f_{(E2P)_2}{}^{max}\right)\frac{[ATP]}{K_A + [ATP]} \quad (1)$$

where $f_{(E2P)_2}{}^{max}$ and $f_{(E2P)_2}{}^{min}$ represent values of $f_{(E2P)_2}$ when no ATP is bound to the $(E2P)_2$ state and when it is saturated by ATP, respectively. K_A represents an ATP dissociation constant for allosteric binding of ATP to the $(E2P)_2$ state. The total fluorescence, F, is due to contributions from fluorescence levels, f, of the probe associated with each of the enzyme conformational states. Because the addition to the enzyme of ATP alone in the absence of Mg^{2+} ions was found to cause only minor fluorescence changes in comparison to that caused by phosphorylation, we assume that the fluorescence levels of all E1 states, i.e., E1:E1, E1ATP:E1, and $(E1ATP)_2$, are all the same. The total fluorescence is then given by

$$F = f_{E1}([E1:E1] + [E1ATP:E1] + [(E1ATP)_2]) + f_{E2P}[E2P:E1] + f_{(E2P)_2}[(E2P)_2] \quad (2)$$

$[(E2P)_2]$ refers here to the sum of the concentrations in the $(E2P)_2$ and $(E2P)_2ATP$ states. The change in fluorescence due to ATP binding is accounted for by eq 1. In this possible interpretation of the fluorescence data the rate constant, k_{-4}, for dephosphorylation of the enzyme in the E2P state and its conversion back into the E1 state (i.e., $(E2P)_2 \rightarrow (E1ATP)_2$ or $(E2P)_2ATP \rightarrow (E1ATP)_2$) can be assumed to be constant with a value for the pig kidney enzyme of 5 s^{-1} (*22*). All of the differential rate equations and all of the other values of the rate constants and equilibrium constants used for modeling the data are exactly the same as previously described (*24*) (see Table 1), and the kinetic scheme shown in Figure 3 is still valid. The fluorescence levels used for simulations based on the model were f_{E1} = 1.0, f_{E2P} = 1.53, $f_{(E2P)_2}{}^{max}$ = 2.06, and $f_{(E2P)_2}{}^{min}$ = 1.80. f_{E1} has been arbitrarily defined as 1.0 as a reference point for the fluorescence changes. f_{E2P} has been chosen to be exactly midway between the values of f_{E1} and $f_{(E2P)_2}{}^{max}$. The values of $f_{(E2P)_2}{}^{max}$ and $f_{(E2P)_2}{}^{min}$ have been chosen to agree with the experimentally observed $\Delta F/F_0$ values at 20 and 500 μM ATP, respectively.

Simulations based on this revision of the dimer model are shown in Figure 2 (solid curve). There it can be seen that this model reproduces the observed experimental behavior just as well or even better than the model in its original form involving ATP-induced acceleration of dephosphorylation described previously (*24*). Therefore, based on the data shown in Figure 2, it is possible to conclude that ATP does in fact bind to the E2P phosphoenzyme of the Na^+,K^+-ATPase, but it is not possible to conclude whether or not this ATP binding has any effect on the normal physiological dephosphorylation of the enzyme. To decide this latter point requires further independent experiments, which will be described shortly.

Fluorescence Amplitudes of Rabbit Na^+,K^+-ATPase. The values of $\Delta F/F_0$ for enzyme from rabbit kidney were measured in a steady-state spectrofluorometer as described under Materials and Methods. The use of a spectrofluorophotometer rather than a stopped-flow spectrofluorometer precludes measurements at ATP concentrations < 0.1 μM, because at such low concentrations the rapid consumption of the ATP causes an immediate drop in fluorescence following the initial rise due to E2P formation. However, the decrease in $\Delta F/F_0$ observed for the pig kidney preparation (see Figure 2) only begins at an ATP concentration of approximately 20 μM. At the enzyme concentrations used in this study the complete consumption of > 20 μM requires minutes to hours, and as such, the mixing of solutions in a steady-state spectrofluorophotometer is perfectly adequate to accurately measure $\Delta F/F_0$ in this ATP concentration range.

The results obtained are shown in Figure 4. As in the case of the pig enzyme, a drop in $\Delta F/F_0$ was observed at high ATP

Table 1: Values of Rate Constants, Equilibrium Constants, and Fluorescence Parameters of the Dimer Model Used for Simulations (Solid Lines) Shown in Figures 2, 4, and 5

parameter	reaction[a]	pig	rabbit	shark
k_1 (μM^{-1} s^{-1})	E1 + ATP → E1ATP	52	52	52
k_{-1} (s^{-1})	E1ATP → E1 + ATP	13	13	13
k_2 (μM^{-1} s^{-1})	E1ATP + ATP → $(E1ATP)_2$	52	52	52
k_{-2} (s^{-1})	$(E1ATP)_2$ → E1ATP + ATP	364	364	364
k_3 (s^{-1})	E1ATP → E2P	15	20	1
k_{-3} (s^{-1})	E2P → E1ATP	5	5	5
k_4 (s^{-1})	$(E1ATP)_2$ → $(E2P)_2$	173	173	173
k_{-4} (s^{-1})	$(E2P)_2$ → $(E1ATP)_2$ and $(E2P)_2ATP$ → $(E1ATP)_2$	5	5	5
K_A (μM)	$(E2P)_2ATP$ ↔ $(E2P)_2$ + ATP	143	500	500
f_{E1}	fluorescence level of E1, E1ATP, and $(E1ATP)_2$	1.0	1.0	1.0
f_{E2P}	fluorescence level of E2P	1.53	1.35	1.3
$f_{(E2P)_2}^{max}$	fluorescence level of $(E2P)_2$	2.06	1.7	2.2
$f_{(E2P)_2}^{min}$	fluorescence level of $(E2P)_2ATP$	1.80	1.5	1.7

[a]For each reaction Na^+ ions have been omitted for simplicity, but in each case the rate constant refers to the value in the presence of 130 mM NaCl. Under such conditions all of the E1 states, with or without ATP, would be completely saturated with Na^+ ions and would, thus, all have three bound Na^+ ions. Also for simplicity, the dimeric nature of each enzyme species has been omitted. Thus, E1 actually represents a dimer E1:E1, where each E1 monomer can only bind a single ATP molecule.

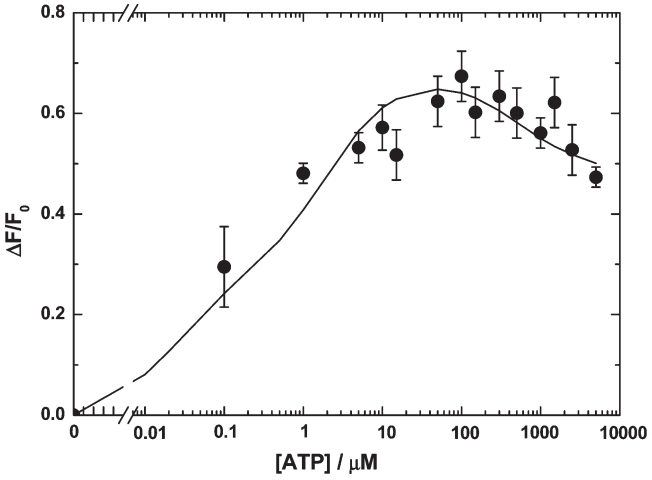

FIGURE 4: Amplitudes ($\Delta F/F_0$) of the total observed fluorescence change caused by the addition of varying concentrations of Na_2ATP to Na^+,K^+-ATPase-containing membrane fragments from rabbit noncovalently labeled with RH421. The Na^+,K^+-ATPase and RH421 concentrations were 9 μg/mL (or 61 nM) and 200 nM. The enzyme suspension and the Na_2ATP stock solution were prepared in a buffer containing 130 mM NaCl, 30 mM imidazole, 5 mM $MgCl_2$, and 1 mM EDTA (pH 7.4, 24 °C). The fluorescence of membrane-bound RH421 was measured at λ_{ex} = 570 nm and λ_{em} = 670 nm. The solid line represents the prediction of simulations based on the dimer model shown in Figure 3.

concentrations. The experimental data could be reproduced by the same dimer kinetic model as used for the pig enzyme. The only parameter values which differed from those used for the pig enzyme were K_A = 500 μM, k_3 = 20 s^{-1}, f_{E2P} = 1.35, $f_{(E2P)_2}^{max}$ = 1.7, and $f_{(E2P)_2}^{min}$ = 1.5 (see Table 1). The fact that the fluorescence levels are different from those of the pig enzyme is not a major concern, because these depend on the purity of the enzyme preparation as well as on the lipid composition and can thus vary from one preparation to another, even for the same source of enzyme. The rabbit enzyme appears to have a somewhat lower ATP affinity for its E2P state than the pig enzyme; i.e., $K_A \approx 500$ μM for the rabbit versus approximately 140 μM for the pig. However, the dependence of $\Delta F/F_0$ on the ATP concentration in the high ATP concentration range is particularly influenced by the values of both K_A and $f_{(E2P)_2}^{min}$. Because $\Delta F/F_0$ would only reach the limiting value of $f_{(E2P)_2}^{min}$ at extremely high ATP concentrations, the value of $f_{(E2P)_2}^{min}$ is not very well defined. For this reason a range of K_A values in the order of hundreds of micromolar could equally well reproduce the experimental behavior. The value of k_3 for the rabbit of 20 s^{-1} is slightly higher than that used to reproduce the pig data (15 s^{-1}). This indicates that the state E1ATP:E1 is slightly easier to phosphorylate in the rabbit than the pig. The low rate constant for this reaction relative to that of a dimer saturated with ATP (E1ATP:E1ATP → E2P:E2P), where the rate constant is close to 200 s^{-1}, has been attributed to interactions between neighboring pump molecules in their membrane which inhibit phosphorylation (*1*). Therefore, the small difference in the values of k_3 for the rabbit and pig enzymes could easily be accounted for by differences in the degree of protein−protein interactions in these two preparations. The slightly higher value of k_3 in the rabbit enzyme is consistent with weaker steric inhibition, which could be due to the enzyme molecules being less closely packed within the membrane than in the case of the pig enzyme or due to a less open E1 conformation in the rabbit relative to the pig enzyme.

Fluorescence Amplitudes of Shark Na⁺,K⁺-ATPase. The values of $\Delta F/F_0$ for enzyme from shark rectal gland were also measured in a steady-state spectrofluorophotometer as described under Materials and Methods. The results obtained for the shark enzyme are shown in Figure 5. As in the case of the pig and rabbit enzymes, a drop in $\Delta F/F_0$ was observed at high ATP concentrations. However, in comparison to the pig and rabbit enzyme preparations the rise in $\Delta F/F_0$ at low concentrations occurred over a significantly smaller ATP concentration range; i.e., there is a steeper rise in $\Delta F/F_0$ with increasing ATP concentration. Whereas the increase in $\Delta F/F_0$ from zero to its maximum value stretches over an ATP concentration of 4 orders of magnitude for the pig and rabbit enzymes, for the shark enzyme it occurs over only approximately 2 orders of magnitude. The slow increase of the pig and rabbit enzymes has been attributed to negative cooperativity in ATP binding to a protein dimer (*24*). Therefore, the steeper increase in $\Delta F/F_0$ for the shark enzyme could be an indication that there is no negative cooperativity in ATP binding in this enzyme and that it exists in the membrane as a monomer. Therefore, in the case of the shark enzyme we have attempted to reproduce the experimental data

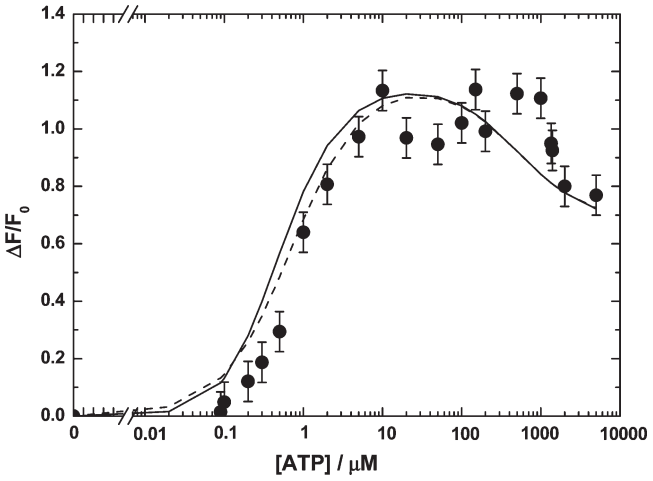

FIGURE 5: Amplitudes ($\Delta F/F_0$) of the total observed fluorescence change caused by the addition of varying concentrations of Na_2ATP to shark Na^+,K^+-ATPase-containing membrane fragments noncovalently labeled with RH421. The Na^+,K^+-ATPase and RH421 concentrations were 6.8 μg/mL (or 46 nM) and 150 nM. The enzyme suspension and the Na_2ATP stock solution were prepared in a buffer containing 130 mM NaCl, 30 mM imidazole, 5 mM $MgCl_2$, and 1 mM EDTA (pH 7.4, 24 °C). The fluorescence of membrane-bound RH421 was measured at λ_{ex} = 577 nm (+OG530 glass cutoff filter) and λ_{em} = 670 nm (+RG645 glass cutoff filter). The solid line and the dashed line represent the predictions of simulations based on the dimer model (shown in Figure 3) and a monomer model, respectively.

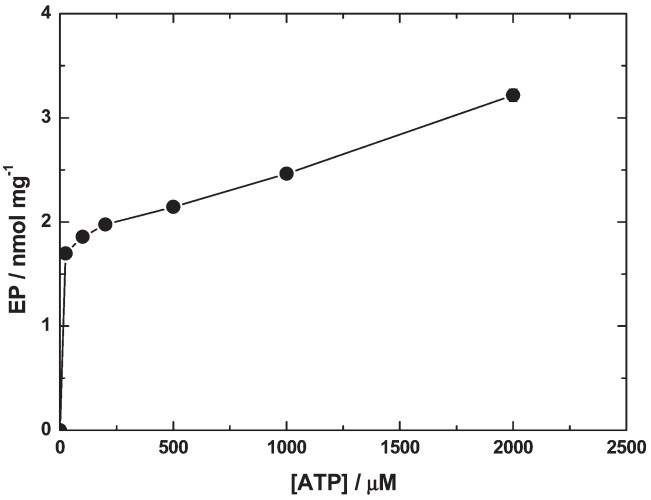

FIGURE 6: Level of phosphoenzyme (EP) of shark Na^+,K^+-ATPase as a function of ATP concentration. The maximum phosphoenzyme levels in the presence of 150 mM NaCl (total EP) were determined as described under Materials and Methods. The standard deviations on the points are covered by the data symbols.

using both the same dimer kinetic model as used for the pig and rabbit enzymes as well as with a monomer model.

As shown in Figure 5 both models were able to reproduce the observed behavior. Therefore, for this particular enzyme there is no reason to prefer a dimer model over a monomer model. At low ATP concentrations (< 1 μM) the experimental date points are consistently shifted to the right of the simulated curves (i.e., to higher ATP concentrations) for both the monomeric and dimeric models. This is most likely due to consumption of ATP during the course of the measurement, so that the actual ATP concentration in the cuvette is lower than the concentration used for the plot. This problem did not occur in the case of the pig kidney data shown in Figure 2 because of rapid mixing in the stopped-flow apparatus, which allows resolution of the kinetics and determination of the value of $\Delta F/F_0$ from an extrapolation of a fit of the experimental transient to infinite time. At high ATP concentrations the simulations of the shark enzyme data based on the two models converge because the phosphorylating ATP site or sites are fully saturated under these conditions, regardless of the model. The only differences between the two models are in the low ATP concentration range (< 10 μM). The one-site monomer model used is the same as that described previously (*24*), except that the drop in $\Delta F/F_0$ has now been described by a drop in the fluorescence level of the E2P state due to ATP binding to the phosphoenzyme in an analogous fashion to the dimer model used here to explain the pig and rabbit data (see eq 1). The expression for f_{E2P} used was thus

$$f_{E2P} = f_{E2P}{}^{max} + \left(f_{E2P}{}^{min} - f_{E2P}{}^{max}\right)\frac{[ATP]}{K_A + [ATP]} \quad (3)$$

In the monomer model the total fluorescence, F, is given by

$$F = f_{E1}([E1] + [E1ATP]) + f_{E2P}[E2P] \quad (4)$$

For the simulations based on the monomer model the only values which varied from those previously published (*24*) were K_{A1} = 25 μM, K_A = 500 μM, $f_{E2P}{}^{max}$ = 2.2 and $f_{E2P}{}^{min}$ = 1.7. K_{A1} is the dissociation constant of ATP with the E1 state of the enzyme. The value of K_A is identical to the value used for the simulations of the rabbit data. Its estimated value of 500 μM is of the same order of magnitude as the K_d estimated for ATP binding to the E2 state of enzyme from the same source, i.e., 184 μM (*42*).

The simulations shown in Figure 5 which were based on the dimer model were performed using the following values of the parameters: K_A = 500 μM, k_3 = 1 s^{-1}, f_{E2P} = 1.3, $f_{(E2P)_2}{}^{max}$ = 2.2, and $f_{(E2P)_2}{}^{min}$ = 1.7. All other parameters used were exactly the same as for the pig enzyme (see Table 1). The major difference in the values of the parameters used between the shark enzyme and the pig and rabbit enzymes is that for the shark one needs to assume a much lower phosphorylation rate constant, k_3, when only one monomer within a dimer has bound ATP; i.e., the rate constant for the reaction E1ATP:E1 → E2P:E1 was taken to be only 1 s^{-1} for the simulation shown in Figure 5 whereas values of 15 s^{-1} and 20 s^{-1} were used for the pig and rabbit, respectively. This indicates that, if the shark enzyme is dimerized, it would have to be very difficult to phosphorylate it until both phosphorylating ATP binding sites within the dimer are occupied.

Although the data presented here do not allow a definitive decision as to whether the shark rectal gland enzyme is actually dimeric or monomeric at low ATP concentrations, on the basis of the grounds of simplicity we would tend to prefer the monomeric model for this enzyme source. If this is the case, then the kinetics and the mechanism of the Na^+,K^+-ATPase would be dependent on the enzyme source. We are currently carrying out further studies on both shark rectal gland and pig kidney enzyme to resolve the question of their state of oligomerization.

Phosphorylation Levels of Shark Na^+,K^+-ATPase. An independent method of determining the amount of phosphoenzyme formed and the effect of ATP is to measure the degree of incorporation of radioactive phosphorus transferred from radioactively labeled ATP. Experiments employing this method have been carried out as described under Materials and Methods.

Measurements of the total amount of phosphoenzyme (EP) are shown in Figure 6. There is a sharp increase in the level of EP on going from zero ATP to 100 μM because the enzyme cannot be phosphorylated in the absence of ATP. After that one observes

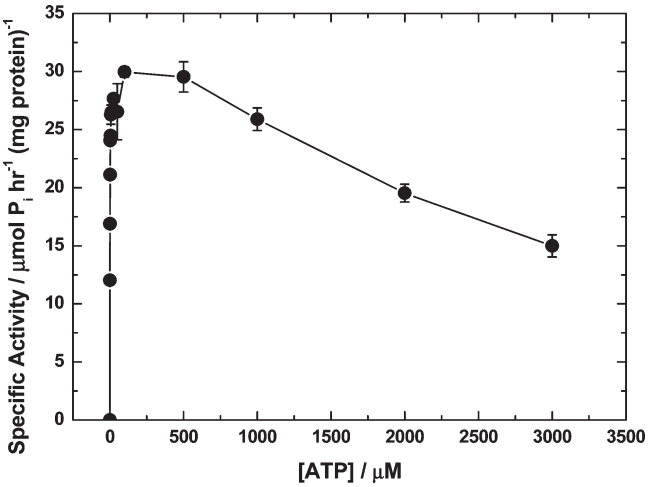

FIGURE 7: Specific Na^+-ATPase activity of shark Na^+,K^+-ATPase as a function of the ATP concentration. The activities were determined at 23 °C as described under Materials and Methods in a buffer containing 130 mM NaCl, 30 mM histidine, 2 mM $MgCl_2$, and 0.033% bovine serum albumin at pH 7.4. The errors on the points represent standard deviations.

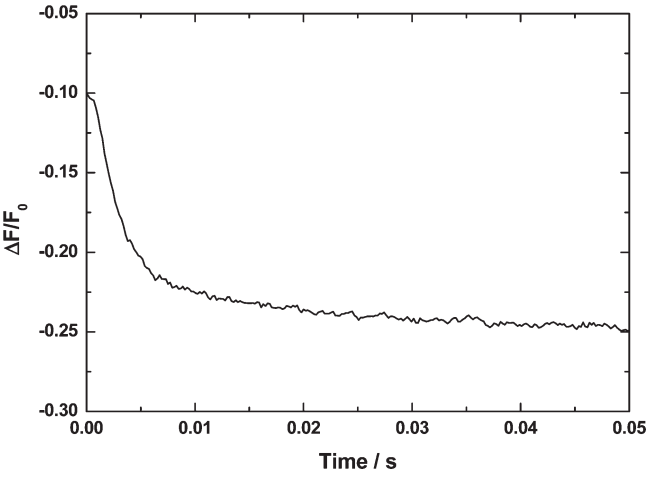

FIGURE 8: Sequential mixing stopped-flow fluorescence transient of Na^+,K^+-ATPase membrane fragments from shark rectal gland noncovalently labeled with RH421. Na^+,K^+-ATPase (20 μg/mL or 135 nM) was premixed with 2.0 mM Na_2ATP. The enzyme was subsequently mixed with an equal volume of a KCl solution (6 mM after mixing). The final Na^+,K^+-ATPase concentration after mixing was 10 μg/mL or 68 nM, and the RH421 concentration after mixing was 150 nM. The enzyme and KCl solutions were in a buffer containing 30 mM imidazole, 130 mM NaCl, 5 mM $MgCl_2$, and 1 mM EDTA, pH 7.4, 24 °C. The fluorescence of membrane-bound RH421 was measured using an excitation wavelength of 577 nm at emission wavelengths ≥665 nm (RG665 glass cutoff filter). The calculated observed rate constants were 364 (±11) s^{-1} (86% of the total amplitude) and 37 (±2) s^{-1} (14% of the total amplitude).

a more gradual increase in the level of phosphoenzyme. The result shown in Figure 6 is in contrast to that shown in Figures 2, 4, and 5, in which a significant drop in fluorescence is observed at ATP concentrations >100 μM. This indicates that the drop in fluorescence at high ATP concentrations shown in Figures 2, 4 and 5 cannot be due to an ATP-induced acceleration of the dephosphorylation, as had previously been suggested (*24*), since this would have to cause a drop in the EP level. Another possible cause for the fluorescence drop could be an ATP-induced change in the degree of Na^+ dissociation from the E2P state.

Effect of ATP on Na^+-ATPase Activity. In the absence of K^+ ions the Na^+,K^+-ATPase is still able to complete its reaction cycle, with Na^+ replacing K^+ as the ion which binds to the E2P state and stimulates dephosphorylation. This overall reaction is termed Na^+/Na^+ exchange or simply Na^+-ATPase activity (*43*). At saturating Na^+ and Mg^{2+} concentrations and ATP concentrations in excess of ~100 μM, it is well established that the rate-determining step of the Na^+-ATPase cycle of the enzyme is the dephosphorylation reaction (*35*, *44*−*46*), which is much more weakly stimulated by Na^+ than the normal physiological ion K^+. Therefore, under these conditions the steady-state turnover number of the enzyme can be considered to be a close approximation to the rate constant of the dephosphorylation reaction. By investigating the effect of high concentrations of ATP (i.e., ≥100 μM) on the enzyme's Na^+-ATPase activity, it is possible to determine whether or not ATP binding to the E2P state has any effect on dephosphorylation.

Results obtained using shark Na^+,K^+-ATPase are shown in Figure 7. At ATP concentrations in the range 0−100 μM one observes a significant increase in activity. At such low ATP concentrations this can be attributed to the stimulation of phosphorylation by ATP. At higher ATP concentrations the data in Figure 7 show a drop in activity. In this concentration range, as stated above, the dephosphorylation reaction is rate-limiting the reaction cycle. Therefore, in agreement with the radioactive measurements of the EP level, the enzyme activity results show no indication of any ATP-induced stimulation of the dephosphorylation reaction. In contrast, it appears that the dephosphorylation reaction is inhibited by millimolar levels of ATP.

K^+-Stimulated Dephosphorylation of the Na^+,K^+-ATPase. To determine whether or not the ATP-induced inhibition of the rate constant of dephosphorylation observed in the Na^+-ATPase mode of the enzyme is also apparent when K^+ is present, measurements of the observed rate constant of dephosphorylation were performed via stopped flow by rapidly mixing phosphorylated shark rectal gland enzyme with either 12, 2, or 0.5 mM KCl as described under Materials and Methods. At 12 mM KCl the observed kinetic traces of the RH421 fluorescence showed a drop in fluorescence which could be well fitted by a biexponential function (see Figure 8). No significant change in the values of the observed rate constants were found over the entire ATP concentration range of 25−3500 μM. Averaging over this entire ATP concentration range, the faster phase (79−88% of the total amplitude) was found to have an observed rate constant of 419 (±42) s^{-1}, and the slower phase (12−21% of the total amplitude) was found to have an observed rate constant of 50 (±9) s^{-1}. The value of the observed rate constant for the faster phase agrees well with the value previously obtained for pig kidney enzyme (*35*) and can be attributed to K^+ binding to the phosphorylated E2P state of the enzyme and consequent stimulation of dephosphorylation (see the Discussion for a more detailed explanation). The slower phase is most likely due to the actual dephosphorylation reaction itself, which because it is directly coupled to the K^+-E2P binding equilibrium would also lead to a drop in fluorescence because it would perturb the binding equilibrium toward the K^+ bound state, $E2P(K^+)_2$. The value of the observed rate constant for the slower phase of 50 (±9) s^{-1} is also consistent with direct measurements of the kinetics of K^+-stimulated dephosphorylation via quenched flow on enzyme from the same source. Although in previous measurements of the dephosphorylation the kinetics appeared to be multiphasic, significant components of the observed transients have been reported with observed rate

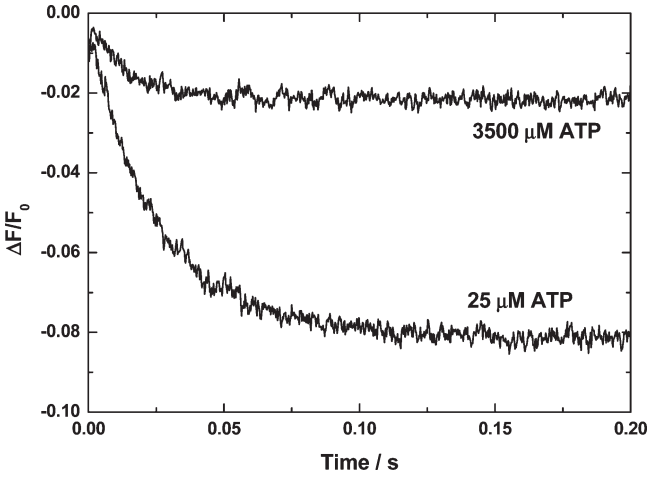

FIGURE 9: Sequential mixing stopped-flow fluorescence transients of Na^+,K^+-ATPase from shark rectal gland. The enzyme was premixed with either 50 or 7000 μM Na_2ATP. It was subsequently mixed with an equal volume of a KCl solution (0.25 mM after mixing). The final ATP concentrations were hence 25 and 3500 μM. The calculated observed rate constants were 72 ($\pm$5) s^{-1} (25 μM ATP) and 39.6 ($\pm$0.7) s^{-1} (3500 μM ATP). All other experimental conditions were as described in Figure 8.

constants of 23 s^{-1} (*36*) and 38.7 s^{-1} (*47*) at 0 °C. At 10 °C Cornelius et al. (*48*) observed monoexponential relaxation kinetics for the K^+-stimulated dephosphorylation of shark enzyme reconsitituted into di-18:1 phosphatidylcholine vesicles with 40% cholesterol with an observed rate constant of 28.7 s^{-1}. The higher value we have measured here could simply be explained by the higher temperature of 24 °C.

In the case of the experiments performed in which the phosphorylated enzyme was mixed with 2 mM KCl, again no significant change in the observed kinetics was apparent on increasing the ATP concentration (after mixing) from 25 to 3500 μM, and the observed rate constants for the two phases of the fluorescence change were in the same ranges as those measured on mixing with 12 mM. This is somewhat surprising, because based on previous measurements of the dephosphorylation kinetics of pig kidney enzyme (*35*) a KCl of 2 mM (or 1 mM after mixing) should be nonsaturating, and therefore, one would have expected a significant drop in the observed rate constants. A possible explanation for this could be that the shark enzyme has a higher affinity for extracellular K^+ ions than the pig enzyme. This is an interesting observation which requires further investigation.

In contrast to the experiments performed by mixing with 12 or 2 mM KCl, when the enzyme was mixed with 0.5 mM KCl (0.25 mM after mixing), a marked difference in the kinetics was observed when the phosphorylation was induced by premixing with 50 or 7000 μM ATP, i.e., final ATP concentrations of 25 and 3500 μM (see Figure 9). At 3500 μM ATP the amplitude of the fluorescence change is only about a quarter of that observed at 25 μM. This result is consistent with a significantly lower level of net K^+ binding to the phosphoenzyme at the higher ATP concentration. The fact that such an effect was not observed at the higher KCl concentrations of 6 and 1 mM (after mixing) can be accounted for by the extracellular K^+ sites being saturated at these concentrations. The measured fluorescence traces at 0.25 mM K^+ (after mixing) could be adequately fitted via a monoexponential time function. The observed rate constants were 39.6 ($\pm$0.7) s^{-1} at 25 μM ATP and 72 ($\pm$5) s^{-1} at 3500 μM ATP. Because the observed rate constant is the sum of the rate constants for K^+ binding to and dissociation from its binding site within the protein matrix, to explain both the decrease in amplitude and the increase in observed rate constant at the higher ATP concentration, one would have to assume that the higher concentration of ATP causes an increase in the rate constant for K^+ dissociation from the phosphoenzyme.

The observed results, therefore, indicate that under physiological conditions, where extracellular K^+ ions would be present at approximately 4 mM (*6*), saturating the K^+ binding sites, the K^+ ions would be expected to abolish the ATP-induced inhibition of dephosphorylation which is observed under K^+-free conditions.

DISCUSSION

The analysis of the amplitudes of stopped-flow kinetic measurements we have presented here supports the conclusion that ATP binds to the E2P form of the Na^+,K^+-ATPase with a dissociation constant in the range 140−500 μM depending on the enzyme source. Steady-state kinetic measurements of Na^+-ATPase activity and radioactive measurements of the phosphoenzyme level indicate that in the absence of K^+ ions ATP binding to the E2P state has a decelerating effect on dephosphorylation of the enzyme along the normal physiological pathway to E2.

Our conclusion that ATP does in fact bind to the phosphoenzyme of the Na^+,K^+-ATPase is in agreement with the findings of Askari and Huang (*17*). However, the effect found here of ATP on the dephosphorylation reaction cannot be directly compared with the results of Askari and Huang because of different experimental procedures and conditions. In our experiments we were measuring the dephosphorylation of phosphoenzyme which had been formed by phosphoryl transfer from ATP, i.e., via the normal physiological route. The dephosphorylation reaction which we have found to be decelerated by ATP is, thus, the normal physiological dephosphorylation reaction E2P → E2. In contrast, Askari and Huang (*17*) formed their phosphoenzyme via a direct phosphorylation by inorganic phosphate (often called "back-door" phosphorylation). Importantly for the discussion here, they found that the rate constant for dephosphorylation of phosphoenzyme formed in this fashion was completely unaffected by the presence of K^+ ions, which is in stark contrast to the physiological dephosphorylation of E2P, which is significantly accelerated by K^+ (*35*, *44*−*46*). Therefore, the dephosphorylation pathway followed in the experiments of Askari and Huang (*17*) must be different from the physiological one studied here. Askari and Huang (*17*) in fact pointed this out themselves. They also pointed out that the phosphoenzyme formed by reaction with inorganic phosphate is known to be capable of being converted by Na^+ to the E1P state (*17*). The dephosphorylation reaction they measured was, therefore, most likely a dephosphorylation of E1P, not E2P.

Since E1P is able to donate its phosphate to ADP and resynthesize ATP (*49*), Askari and Huang (*17*) suggested that the role ATP binding to the phosphoenzyme of the Na^+,K^+-ATPase plays in the enzyme's mechanism is to inhibit ATP synthase activity, i.e., to keep the enzyme running forward as a pump rather than consuming the energy of the Na^+ electrochemical potential gradient across the membrane, which it has just created, by resynthesizing ATP. By binding preferentially to the E2P form of the enzyme, ATP could effectively do this by shifting the E1P ↔ E2P equilibrium in the direction of E2P. This interpretation is, furthermore, consistent with other studies showing that high concentrations of ATP inhibit the synthesis of ATP by the Na^+,K^+-ATPase (*50*, *51*).

The fact that ATP binding to the E2P state of the Na^+,K^+-ATPase causes a reduction of the fluorescence level of RH421 associated with this state requires some explanation. To account for this drop in $\Delta F/F_0$ observed at high ATP concentrations via an ATP-induced increase in the dephosphorylation rate constant (see Figure 2), it was found that an increase from 5 s^{-1} to 75 s^{-1} was required, i.e., a 25-fold increase. Such a huge increase in rate constant is not compatible with the specific activity results. Therefore, the previous interpretation (*24*) of the drop in the amplitude of the RH421 fluorescence increase at high ATP concentrations as being due to an increase in the dephosphorylation rate constant must be discarded. We conclude that the kinetic model described earlier whereby ATP modifies the fluorescence level of RH421 associated with the E2P state provides a better description of the experimental behavior. The increase in fluorescence of RH421 due to the formation of E2P has been attributed to the release of Na^+ ions from within the protein matrix (*40*, *46*, *52*), which results in a change in the intramembrane electric field detected by the voltage-sensitive probe, either from the release of the ions themselves, a simultaneous movement of charged amino acid residues, or the displacement of charged or dipolar lipid residues around the protein accompanying Na^+ release. A possible interpretation of the drop in fluorescence level of the E2P state at high ATP concentrations could then be that ATP is causing Na^+ rebinding or an inhibition of Na^+ release, so that in the steady state the distribution of enzyme between the states $E2P(Na^+)_3$, $E2P(Na^+)_2$, $E2PNa^+$, and E2P is shifted toward Na^+-bound states when ATP is simultaneously bound. This could perhaps be tested by voltage-jump measurements (e.g., on enzyme in squid axons or expressed in oocytes), which allow electrical transients associated with Na^+ release from the E2P state to be kinetically resolved (*53*).

In the Na^+-ATPase mode of activity $2Na^+$ replace the $2K^+$ ions that normally bind from the extracellular solution and stimulate dephosphorylation. Nevertheless, one Na^+ must still dissociate prior to dephosphorylation. If ATP is causing an inhibition of dissociation of this third Na^+ ion, this could explain the drop in Na^+-ATPase activity (see Figure 7) and the increase in the steady-state phosphoenzyme level (see Figure 6) experimentally observed in the millimolar ATP concentration range. If further information on the equilibrium constants for Na^+ release from the E2P state becomes available, this effect could be included in the kinetic model in future.

In contrast to the ATP-induced inhibition of dephosphorylation in the Na^+-ATPase mode of the enzyme, the stopped-flow results presented here indicate that no inhibition of dephosphorylation by ATP would be expected in the physiological Na^+,K^+-ATPase mode of the enzyme under normal physiological conditions when approximately 4 mM K^+ is present in the extracellular medium and 120 mM in the cytoplasm (*6*). A possible explanation for this could be that, when the K^+ concentration is in the millimolar range, the K^+ ions can so effectively displace Na^+ from E2P that the inhibitory effect of ATP on dephosphorylation observed under K^+-free conditions is completely overcome. A significant ATP-induced reduction in net K^+ binding was, however, observed at the nonsaturating K^+ concentration of 0.25 mM. This is consistent with a blockage of the transport sites by Na^+ ions at high ATP concentrations, as described above for K^+-free conditions. The time courses of fluorescence transients observed at 0.25 mM K^+ suggested that ATP bound to the phosphoenzyme causes an increase in the rate constant for K^+ dissociation from the extracellular sites. This could perhaps be explained by electrostatic repulsion from Na^+ ions already in the sites. However, because the enzyme preparations used in this study consisted of open membrane fragments, it is not possible to conclude from this work whether the K^+ ion which abolishes ATP inhibition of dephosphorylation is binding from the cytoplasmic or the extracellular surface or whether it is binding to a transport site or to an allosteric site. An allosteric cytoplasmic K^+ site has in fact recently been identified in the crystal structure of the Na^+,K^+-ATPase (*15*, *54*).

The mechanism by which K^+ ions abolish the inhibitory effect of ATP on dephosphorylation cannot be concluded from these studies. However, a feasible hypothesis has been put forward by Fukushima et al. (*11*), who proposed that K^+ binding to the phosphoenzyme causes the dissociation of ATP so that it can no longer inhibit dephosphorylation. A critical analysis of this hypothesis would require binding studies to be performed on the phosphoenzyme under conditions where turnover is not possible.

Finally, it is interesting to discuss the origin of the rapid phase ($\sim$400 s^{-1}) of the drop in RH421 fluorescence following mixing of the phosphorylated enzyme with KCl (see Figure 8). In the Results section it was stated that this could be attributed to K^+ binding to the phosphorylated enzyme stimulating dephosphorylation. However, what is the rate-determining step in this process? In contrast to radioactive-based quenched-flow studies (*54*), which directly determine the formation of dephosphorylated enzyme, the fluorescence stopped-flow measurements described here utilizing the electric field sensitive probe RH421 do not directly detect phosphorylation or dephosphorylation. Instead, it is generally agreed that RH421 detects changes in electric field strength within the protein (*40*, *46*, *52*). Electrophysiological studies (*55*−*57*) have shown that K^+ binding from the extracellular solution to sites within the protein is electrogenic; i.e., it causes a change in electric field strength within the protein. Hence, this is the process which is most likely causing the drop in fluorescence of the probe. This conclusion was already reached in an earlier publication (*58*). However, previous studies (*35*) on the observed rate constant of the rapid phase of the RH421 signal as a function of the K^+ concentration in solution have shown that for pig kidney enzyme it saturates at a K^+ concentration of around 5 mM. This indicates that the fluorescence change is not due to K^+ association to the surface of the protein, since the observed rate constant for such a process should continue to increase linearly with the K^+ concentration. The saturation of the observed rate constant indicates that the rate-determining step leading to the fluorescence change must be a first-order reaction following K^+ association to the protein surface. The results are, thus, consistent with the fluorescence change originating from electrogenic K^+ binding to sites within the protein matrix which is rate-limited by a movement of K^+ ions from the surface of the protein to their final destination at the specific ion binding sites. This movement is in fact a first-order process, since, once the K^+ ions have bound to the protein surface, the rate at which ions traverse the distance from the protein surface only depends on the distance they have to travel, the temperature, and the diffusion coefficient of the ions within the protein. The K^+ concentration in the bulk solution has no effect on the rate of this process. In formal kinetic terms the movement of the K^+ ions within the protein can be seen as a conformational change of a protein−K^+ complex. Such a movement of the K^+ ions is consistent with the widely accepted hypothesis of an "ion well" or "access channel" on the

extracellular face of the protein (*59*). The binding of the K^+ ions to their binding sites within the protein must cause a conformational change on the cytoplasmic side of the enzyme which allows water access to the phosphorylation site, stimulating its dephosphorylation.

Concerning the physiological role of ATP binding to the Na^+,K^+-ATPase phosphoenzyme, because millimolar concentrations of ATP have no effect on the kinetics of the enzyme's dephosphorylation in its physiological Na^+,K^+-ATPase mode, it seems that, if ATP is still bound to the enzyme in the presence of K^+ ions, one advantage could be to stabilize the E2P state and thus to keep the enzymes running in the forward direction, hydrolyzing ATP and pumping ions rather than resynthesizing ATP. ATP binding to the phosphoenzyme of the Na^+,K^+-ATPase would also make good mechanistic sense for the enzyme. It is now known that the enzyme only has a single ATP binding site and that ATP fulfils both allosteric and catalytic functions in different parts of the reaction cycle (*1*, *60*). By binding to the phosphoenzyme as soon as possible after phosphorylation, ATP would, thus, already be present in its site ready to carry out the next phosphorylation reaction in the subsequent turnover of the enzyme's reaction cycle. Therefore, the enzyme would not need to "wait" at any later point in its reaction cycle for ATP to bind so that phosphorylation could occur. This would effectively optimize the turnover number of the enzyme.

ACKNOWLEDGMENT

The authors thank Prof. Helge Rasmussen, Royal North Shore Hospital, Sydney, for financial assistance supporting enzyme transport and Milena Roudna for expert technical assistance.

REFERENCES

1. Clarke, R. J. (2009) Mechanism of allosteric effects of ATP on the kinetics of P-type ATPases. *Eur. Biophys. J. 39*, 3–17.
2. Scheiner-Bobis, G. (2002) The sodium pump. Its molecular properties and mechanics of ion transport. *Eur. J. Biochem. 168*, 123–131.
3. Lüpfert, C., Grell, E., Pintschovius, V., Apell, H.-J., Cornelius, F., and Clarke, R. J. (2001) Rate limitation of the Na^+,K^+-ATPase pump cycle. *Biophys. J. 81*, 2069–2081.
4. Steinberg, M., and Karlish, S. J. D. (1989) Studies of conformational changes in Na,K-ATPase labeled with 5-iodoacetamidofluorescein. *J. Biol. Chem. 264*, 2726–2734.
5. Humphrey, P. A., Lüpfert, C., Apell, H.-J., Cornelius, F., and Clarke, R. J. (2002) Mechanism of the rate-determining step of the Na^+,K^+-ATPase pump cycle. *Biochemistry 41*, 9496–9507.
6. Kong, B. Y., and Clarke, R. J. (2004) Identification of potential regulatory sites of the Na^+,K^+-ATPase by kinetic analysis. *Biochemistry 43*, 2241–2250.
7. Cable, M. B., and Briggs, F. N. (1988) Allosteric regulation of cardiac sarcoplasmic reticulum Ca-ATPase: a comparative study. *Mol. Cell. Biochem. 82*, 29–36.
8. Cable, M. B., Feher, J. J., and Briggs, F. N. (1985) Mechanism of allosteric regulation of the Ca,Mg-ATPase of sarcoplasmic reticulum: studies with 5′-adenylated methylenediphosphate. *Biochemistry 24*, 5612–5619.
9. Champeil, P., and Guillain, F. (1986) Rapid filtration of the phosphorylation-dependent dissociation of calcium from transport sites of purified sarcoplasmic reticulum ATPase and ATP modulation of the catalytic cycle. *Biochemistry 25*, 7623–7633.
10. Clausen, J., McIntosh, D. B., Woolley, D. G., and Andersen, J. P. (2008) Critical interaction of actuator domain residues arginine 174, isoleucine 188, and lysine 205 with modulatory nucleotide in sarcoplasmic reticulum Ca^{2+}-ATPase. *J. Biol. Chem. 283*, 35703–35714.
11. Fukushima, Y., Yamada, S., and Nakao, M. (1984) ATP inactivates hydrolysis of the K^+-sensitive phosphoenzyme of kidney Na^+,K^+-transport ATPase and activates that of muscle sarcoplasmic reticulum Ca^{2+}-transport ATPase. *J. Biochem. 95*, 359–368.
12. Sørensen, T. L.-M., Møller, J. V., and Nissen, P. (2004) Phosphoryl transfer and calcium ion occlusion in the calcium pump. *Science 304*, 1672–1675.
13. Olesen, C., Picard, M., Winther, A.-M. L., Gyrup, C., Morth, J. P., Oxvig, C., Møller, J. V., and Nissen, P. (2007) The structural basis of calcium transport by the calcium pump. *Nature 450*, 1036–1042.
14. Morth, J. P., Pedersen, B. P., Toustrup-Jensen, M. S., Sørensen, T. L.-M., Petersen, J., Andersen, J. P., Vilsen, B., and Nissen, P. (2007) Crystal structure of the sodium-potassium pump. *Nature 450*, 1043–1050.
15. Shinoda, T., Ogawa, H., Cornelius, F., and Toyoshima, C. (2009) Crystal structure of the sodium-potassium pump at 2.4 Å resolution. *Nature 459*, 446–450.
16. Ogawa, H., Shinoda, T., Cornelius, F., and Toyoshima, C. (2009) Crystal structure of the sodium-potassium pump with bound potassium and ouabain. *Proc. Natl. Acad. Sci. U.S.A. 106*, 13742–13747.
17. Askari, A., and Huang, W. (1982) Na^+,K^+-ATPase: evidence for the binding of ATP to the phosphoenzyme. *Biochem. Biophys. Res. Commun. 104*, 1447–1453.
18. Post, R. L., Toda, G., and Rogers, R. N. (1975) Phosphorylation by inorganic phosphate of sodium plus potassium ion transport adenosine triphosphatase. Four reactive intermediates. *J. Biol. Chem. 250*, 691–701.
19. Karlish, S. J. D., and Yates, D. W. (1978) Tryptophan fluorescence of (Na^+ + K^+)-ATPase as a tool for study of the enzyme mechanism. *Biochim. Biophys. Acta 527*, 115–130.
20. Forbush, B., III. (1987) Rapid release of ^{42}K and ^{86}Rb from an occluded state of the Na,K-pump in the presence of ATP or ADP. *J. Biol. Chem. 262*, 11104–11115.
21. Kane, D. J., Fendler, K., Grell, E., Bamberg, E., Taniguchi, K., Froehlich, J. P., and Clarke, R. J. (1997) Stopped-flow kinetic investigations of conformational changes of pig kidney Na^+,K^+-ATPase. *Biochemistry 36*, 13406–13420.
22. Clarke, R. J., Kane, D. J., Apell, H.-J., Roudna, M., and Bamberg, E. (1998) Kinetics of the Na^+-dependent conformational changes of rabbit kidney Na^+,K^+-ATPase. *Biophys. J. 75*, 1340–1353.
23. González-Lebrero, R. M., Kaufman, S. B., Montes, M. R., Nørby, J. G., Garrahan, P. J., and Rossi, R. C. (2002) The occlusion of Rb^+ in the Na^+/K^+-ATPase. *J. Biol. Chem. 277*, 5910–5921.
24. Clarke, R. J., and Kane, D. J. (2007) Two gears of pumping by the sodium pump. *Biophys. J. 93*, 4187–4196.
25. Skou, J. C., and Esmann, M. (1988) Preparation of membrane Na^+, K^+-ATPase from rectal glands of *Squalus acanthias*. *Methods Enzymol. 156*, 43–46.
26. Ottolenghi, P. (1975) The reversible delipidation of a solubilized sodium-plus-potassium ion-dependent adenosine triphosphatase. *Biochem. J. 151*, 61–66.
27. Peterson, G. L. (1977) A simplification of the protein assay method of Lowry et al. which is more generally applicable. *Anal. Biochem. 83*, 346–356.
28. Lowry, O. H., Rosebrough, N. J., Farr, A. L., and Randall, R. J. (1951) Protein measurement with the Folin phenol reagent. *J. Biol. Chem. 193*, 265–275.
29. Jørgensen, P. L., and Andersen, J. P. (1988) Structural basis for E_1-E_2 conformational transitions in Na,K-pump and Ca-pump proteins. *J. Membr. Biol. 103*, 95–120.
30. Fendler, K., Grell, E., Haubs, M., and Bamberg, E. (1985) Pump currents generated by the purified Na^+,K^+-ATPase from kidney on black lipid membranes. *EMBO J. 4*, 3079–3085.
31. Jørgensen, P. L. (1974) Purification and characterization of (Na^+ + K^+)-ATPase III. Purification from the outer medulla of mammalian kidney after selective removal of membrane components by sodium dodecylsulphate. *Biochim. Biophys. Acta 356*, 36–52.
32. Jørgensen, P. L. (1974) Isolation of (Na^+ + K^+)-ATPase. *Methods Enzymol. 32*, 277–290.
33. Schwartz, A., Nagano, K., Nakao, M., Lindenmayer, G. E., Allen, J. C., and Matsui, H. (1971) The sodium- and potassium-activated adenosinetriphosphatase system. *Methods Pharmacol. 1*, 361–388.
34. Nørby, J. G., and Jensen, J. (1971) Binding of ATP to brain microsomal ATPase: determination of the ATP-binding capacity and the dissociation constant of the enzyme-ATP complex as a function of K^+-concentration. *Biochim. Biophys. Acta 233*, 104–116.
35. Kane, D. J., Grell, E., Bamberg, E., and Clarke, R. J. (1998) Dephosphorylation kinetics of pig kidney Na^+,K^+-ATPase. *Biochemistry 37*, 4581–4591.
36. Cornelius, F. (1995) Phosphorylation/dephosphorylation of reconstituted shark Na^+,K^+-ATPase: one phosphorylation site per $\alpha\beta$ protomer. *Biochim. Biophys. Acta 1235*, 197–204.

37. Lindberg, O., and Ernster, L. (1956) Determination of organic phosphorous compounds by phosphate analysis, in Methods in Biochemical Analysis (Glick, D., Ed.) Vol. *3*, pp 1−22, Interscience, New York.
38. Baginski, E. S., Foa, P. P., and B. Zak, B. (1967) Determination of phosphate: Study of labile organic phosphate interference. *Clin. Chim. Acta 15*, 155–158.
39. Cornelius, F. (1999) Rate determination in phosphorylation of shark rectal Na,K-ATPase by ATP: temperature sensitivity and effects of ADP. *Biophys. J. 77*, 934–942.
40. Stürmer, W., Bühler, R., Apell, H.-J., and Läuger, P. (1991) Charge translocation by the Na,K-pump. II. Ion binding and release at the extracellular face. *J. Membr. Biol. 121*, 163–176.
41. Pratap, P. R., and Robinson, J. D. (1993) Rapid kinetic analyses of the Na^+/K^+-ATPase distinguish among different criteria for conformational change. *Biochim. Biophys. Acta 1151*, 89–98.
42. Cornelius, F., Mahmmoud, Y. A., Meischke, L., and Cramb, G. (2005) Functional significance of the shark Na,K-ATPase N-terminal domain. Is the structurally variable N-terminus involved in tissue-specific regulation by FXYD proteins? *Biochemistry 44*, 13051–13062.
43. Cornelius, F. (1991) Functional reconstitution of the sodium pump. Kinetics of exchange reactions performed by reconstituted Na/K-ATPase. *Biochim. Biophys. Acta 1071*, 19–66.
44. Campos, M., and Beaugé, L. (1992) Effects of magnesium and ATP on pre-steady state phosphorylation kinetics of the Na^+,K^+-ATPase. *Biochim. Biophys. Acta 1105*, 51–60.
45. Hobbs, A. S., Albers, R. W., and Froehlich, J. P. (1980) Potassium-induced changes in phosphorylation and dephosphorylation of ($Na^+ + K^+$)-ATPase observed in the transient state. *J. Biol. Chem. 255*, 3395–3402.
46. Apell, H.-J., Roudna, M., Corrie, J. E. T., and Trentham, D. R. (1996) Kinetics of the phosphorylation of Na,K-ATPase by inorganic phosphate detected by a fluorescence method. *Biochemistry 35*, 10922–10930.
47. Cornelius, F., Fedosova, N. U., and Klodos, I. (1998) E2P phosphoforms of Na,K-ATPase. II. Interaction of substrate and cation-binding sites in Pi phosphorylation of Na,K-ATPase. *Biochemistry 37*, 16686–16696.
48. Cornelius, F., Turner, N., and Christensen, H. R. Z. (2003) Modulation of Na,K-ATPase by phospholipids and cholesterol. II. Steady-state and presteady-state kinetics. *Biochemistry 42*, 8541–8549.
49. Post, R. L., Taniguchi, K., and Toda, G. (1974) Synthesis of adenosine triphosphate by Na^+,K^+-ATPase. *Ann. N.Y. Acad. Sci. 242*, 80–90.
50. Blostein, R. (1975) Na^+ ATPase of the mammalian erythrocyte membrane. Reversibility of phosphorylation at 0°. *J. Biol. Chem. 250*, 6118–6124.
51. Robinson, J. D. (1976) The ($Na^+ + K^+$)-dependent ATPase. Mode of inhibition of ADP/ATP exchange activity by $MgCl_2$. *Biochim. Biophys. Acta 440*, 711–722.
52. Klodos, I. (1994) Partial reactions in Na^+/K^+- and H^+/K^+-ATPase studied with voltage-sensitive fluorescent dyes, in The Sodium Pump: Structure Mechanism, Hormonal Control and Its Role in Disease (Bamberg, E., and Schoner, W., Eds.) pp 517−528, Steinkopff Verlag, Darmstadt, Germany.
53. Yaragatupallai, S., Olivera, J. F., Gatto, C., and Artigas, P. (2009) Altered Na^+ transport after an intracellular α-subunit deletion reveals strict external sequential release of Na^+ from the Na/K pump. *Proc. Natl. Acad. Sci. U.S.A. 106*, 15507–15512.
54. Schack, V. R., Morth, J. P., Toustrup-Jensen, M. S., Anthonisen, A. N., Nissen, P., Andersen, J. P., and Vilsen, B. (2008) Identification and function of a cytoplasmic K^+ site of the Na^+,K^+-ATPase. *J. Biol. Chem. 283*, 27982–27990.
55. Bielen, F. V., Glitsch, H. G., and Verdonck, F. (1991) Dependence of Na^+ pump current on external monovalent cations and membrane potential in rabbit cardiac Purkinje cells. *J. Physiol. 442*, 169–189.
56. Rakowski, R. F., Vasilets, L. A., LaTona, J., and Schwarz, W. (1991) A negative slope in the current-voltage relationship of the Na^+/K^+ pump in *Xenopus* oocytes produced by reduction of external [K^+]. *J. Membr. Biol. 121*, 177–187.
57. Peluffo, R. D., and Berlin, J. R. (1997) Electrogenic K^+ transport by the Na^+-K^+ pump in rat cardiac ventricular myocytes. *J. Physiol. 501*, 33–40.
58. Bühler, R., and Apell, H.-J. (1995) Sequential potassium binding at the extracellular side of the Na,K-pump. *J. Membr. Biol. 145*, 165–173.
59. Läuger, P., and Apell, H.-J. (1986) A microscopic model for the current-voltage behaviour of the Na,K-pump. *Eur. Biophys. J. 13*, 305–321.
60. Clarke, R. J., Apell, H.-J., and Kong, B. Y. (2007) Allosteric effect of ATP on Na^+,K^+-ATPase conformational kinetics. *Biochemistry 46*, 7034–7044.